GPS Solutions (2024) 28:173
https://doi.org/10.1007/s10291-024-01717-4

ORIGINAL ARTICLE

A preliminary result for centralized autonomous orbit determination of gnss constellation and lunar satellite based on inter-satellite link measurements

Peng Luo[1,2] · Ye-Zhi Song[1,2] · Jianhua Yang[1] · Xiaogong Hu[1,2] · Chengpan Tang[1,2] · Kai Li[1,2] · Qingfeng Wu[1,3]

Received: 5 March 2024 / Accepted: 22 July 2024

Abstract
The Inter-Satellite Link (ISL) technology plays a vital role in BeiDou Navigation Satellite System (BDS), and it's a developmental trend of the future GNSS. However, ISL is insensitive to both the Earth's rotation and the constellation's overall rotation, which has resulted in persistent overall constellation drift issues for autonomous navigation. Due to technical limitations, the current method for autonomous navigation requires adding ground anchor stations in order to connect the satellite constellation to Earth's surface, thereby minimizing the drift of constellation. Nevertheless, this approach is not a fully autonomous navigation as we expected. This paper proposes an autonomous navigation scheme based on ISL utilizing a lunar satellite as a spatial anchor point and leveraging lunar gravity to establish an inertial space direction reference for the satellite constellation. The feasibility and effectiveness of this scheme are validated through theoretical analysis and simulation experiments. After 120 days of precise orbit determination simulation, the accuracy of result is improved from 408.56 m to 7.78 m, which shows a 98% improvement for all GNSS orbit by adding a lunar satellite into ISL net. This improvement is primarily observed in terms of tangent and normal directions, which experience enhancements of 89.6% and 98.6%, respectively. Specifically, we achieve an improvement of approximately 89% in the accuracy of the inclination angle, around 99% in the right ascension of ascending node, and about 89% in the sum of the argument of perigee and mean anomaly.

Keywords Inter-satellite link · Autonomous navigation · Precise orbit determination · GNSS · Lunar satellite

Introduction

The Inter Satellite Link (ISL) technology plays a vital role in the BeiDou Navigation Satellite System (BDS) providing global high-precision Position, Navigation, and Timing (PNT) services(Li et al. 2023; Yang et al. 2023b). The stability and reliability of Global Navigation Satellite System (GNSS) services are enhanced by ISL, allowing for precise verification of general relativity and related theories(Yang et al. 2023a). ISL will soon become vital for constructing various GNSS systems(Xie et al. 2019).

In addition, ISL technology also plays a crucial role in achieving autonomous navigation of satellites in special circumstances. Markley(Markley 1984) proposed that inter-satellite relative measurements, such as range, angle, and attitude measurement, which could be utilized to determine the orbit of two Earth satellites. Psiaki(Psiaki 1999) researched the orbit determination problem based on relative position data. He suggested that the inter-satellite measurement of two satellites was equivalent to a single-axis gravity gradient instrument with a more extended baseline. The difference in gravity gradient causes a change in relative motion, which explains the feasibility of determining the absolute position of the satellite based on relative motion measurement. Tang et al. (Tang et al. 2017)performed a centralized autonomous orbit determination experiment by

✉ Ye-Zhi Song
syz@shao.ac.cn

[1] Shanghai Astronomical Observatory, Chinese Academy of Sciences, Shanghai 200030, China

[2] University of Chinese Academy of Sciences, Beijing 100049, China

[3] School of Physics and Astronomy, China West Normal University, Nanchong 637002, China

Published online: 07 August 2024

utilizing Ka-band ISL data of BDS-3 in conjunction with a ground anchor station. The radial error between the result and the 24-hour forecasted orbit was better than 10 cm, and the three-dimensional position error was better than 1.5 m.

Despite the remarkable advancements in autonomous navigation through ISL, a significant technical challenge remains unresolved. The persistent issue of constellation overall rotation or inaccurate constellation orientation, continues to pose a formidable obstacle. Research conducted by Liu and Liu(Liu and Liu 2001) has demonstrated that the normal equation derived from inter-satellite measurement exhibits rank deficiency within the context of the two-body problem primarily causing imprecise right ascension of the ascending node estimation of the satellite, resulting in an imprecise orientation of its orbit plane. Hill's doctoral thesis(Hill 2007) elucidated the underlying causes behind the pervasive rotational issue encountered by constellations. He posited that relying solely on ISL data was insufficient for determining the orbital state of near-Earth satellites due to the inherent symmetry within Earth's gravitational field proximity. Zhang Yan(Zhang 2005) also analyzed this problem and discovered that ill-conditioned equations of POD could arise for quantities associated with orbital direction such as orbital inclination, argument of perigee, and right ascension of ascending node of the satellite. To address this issue, several scholars have proposed incorporating ground anchor stations into their approaches. Tang(Tang et al. 2018) and others have tested this method and achieved favorable outcomes. It should be noted that adding ground anchor stations to ISL does not constitute a fully autonomous navigation solution.

Exploration of deep space is crucial for humanity to discover the secrets of the universe and pursue sustainable development. The Earth-Moon region represents a significant frontier for such exploration. Hill's analysis(Hill and Born 2007) has indicated that the gravitational field in near-Earth space exhibits high symmetry, posing challenges in accurately orienting satellites with the ISL system. However, deploying one spacecraft from the ISL network in Cislunar space could potentially resolve the rotational issue faced by this constellation. For example, Psiaki(Psiaki 2007) developed a method to estimate the orbits of two satellites along with corrections to the gravity model of the central body using relative position measurements and applied this method on the moon by simulation. Parker and Anderson(Parker et al. 2012) performed LiAISON between a lunar halo orbiter and a GEO satellite, and the simulation results have demonstrated that the absolute positions and velocities of both satellites can be estimated with relative measurements only. Zhang and Xu(Zhang and Xu 2015) developed a virtual lunar exploration scenario to verify the navigation performance of the Earth-Moon L1,2,4,5 four-satellite constellations, using satellite-to-satellite range measurement between the users and Lagrange point navigation satellites. Huang et al.(Huang et al. 2022) performed a simulation of orbit determination of L1,2,4,5, DRO, and MEO in cislunar space using ISL data, but they didn't analyze the performance of resisting the overall constellation drift.

However, these simulations above are mostly based on the three-body problem or a simplified perturbation model, which may lack of substantial practical engineering applicability. Additionally, most simulations are conducted for spacecraft positioned at Lagrange points. However, ensuring stable spacecraft operation at Lagrange points needs continuous orbit maneuvers, presenting significant challenges for Precise Orbit Determination (POD). Conversely, conventional man-made lunar satellites (LunarSat) do not encounter comparable difficulties.

This paper aims to assess the feasibility of the navigation system in the cislunar space, considering the unique challenges faced by the current BDS and future autonomous navigation requirements. We try to add a lunar satellite to the ISL net and use it as a spatial anchor within dynamic constraints of the lunar gravity field. This integration will establish directional benchmarks for the navigation satellite constellation in inertial space, and effectively mitigate overall drift during autonomous navigation. Subsequently, we evaluate the feasibility and effectiveness of this approach through theoretical analysis and simulation.

Methodology

We first present the basic theory of Precise orbit determination based on ISL measurements. Then, the theory of the autonomous navigation based on ISL, which including the rank deficiency in autonomous navigation, the gravitational asymmetric theory and the feasibility analysis of the approach by adding a lunar satellite to the ISL net.

Normalized observations for ISL

The ISL of BDS adopts Time Division Multiple Access (TDMA) technology(Tang et al. 2022). When establishing an ISL between two satellites A and B, they will generate uplink and downlink observation at specific times t_1 and t_2, which can be represented as $\rho_{AB}(t_1)$ and $\rho_{BA}(t_2)$, respectively. To facilitate subsequent data processing, Tang et al.(Tang et al. 2018) employed the prediction results of satellite orbit and clock error to normalize the observation equation for inter-satellite links. As a result, the normalized accuracy of ISL observations can achieve a remarkable

precision of 1 cm. The normalized observation can be expressed as:

$$\begin{aligned}\rho(t_0) &= \frac{\rho_{AB}(t_0)+\rho_{BA}(t_0)}{2} \\ &= |\mathbf{R}_B(t_0)-\mathbf{R}_A(t_0)| + c\cdot X^A_{Delay} + c\cdot X^B_{Delay} \\ &+ \frac{\Delta\rho^{AB}_{cor}+\Delta\rho^{BA}_{cor}}{2}\end{aligned} \tag{1}$$

Where $X^A_{Delay}=\frac{\tau^{send}_A+\tau^{rcv}_A}{2}$ and $X^B_{Delay}=\frac{\tau^{send}_B+\tau^{rcv}_B}{2}$ are the normalized clock error for satellites A and B, respectively. The observation errors $\Delta\rho^{AB}_{cor}$ and $\Delta\rho^{BA}_{cor}$ correspond to the uplink and downlink observation, respectively. In the case of ISL between MEO satellites, the normalized observation accuracy typically reaches up to 1 cm. However, for ISL between MEO satellites and LunarSat, the normalized observation accuracy usually reaches up to 1 m. The observing epoch, denoted as t_0, which is typically selected as either t_1 or t_2.

In this paper, clock error is not considered, and Eq. (1) can be employed to directly simulate and calculate.

Precise orbit determination

The equation of a satellite moving in the cislunar space can be expressed as follows:

$$\ddot{\mathbf{r}} = -GM\frac{\mathbf{r}}{r^3} + \mathbf{f}(\mathbf{r},\dot{\mathbf{r}},\mathbf{p},t) \tag{2}$$

Where $\mathbf{r}$, $\dot{\mathbf{r}}$ and $\ddot{\mathbf{r}}$ are the position, velocity, and acceleration of the satellite's center of mass respectively. $\mathbf{p}$ is the vector of the satellite perturbation coefficient.

The perturbation force acting on the satellite, denoted as $\mathbf{f}$, is the cumulative effect of various perturbations including n-body perturbation, earth's non-spherical gravity field, earth's tidal forces, solar radiation pressure, earth's radiative pressure, relativistic effects, and other factors. In the case of lunar satellites, additional consideration should be given to the moon's non-spherical gravity field.

Let $\mathbf{X}=(\mathbf{r},\dot{\mathbf{r}},\mathbf{p})^T$, then the state equation and initial state of the satellite can be expressed as:

$$\begin{cases}\dot{\mathbf{X}} = \mathbf{F}(\mathbf{X},t) \\ \mathbf{X}|_{t_0} = \mathbf{X}_0\end{cases} \tag{3}$$

Assume a state vector $\mathbf{X}_0$ at an initial epoch is known, and then the initial state $\mathbf{X}^*$ at any epoch t can be obtained through the integration of Eq. (3). The linear expansion of Eq. (3) leads to:

$$\dot{\mathbf{X}} = \dot{\mathbf{X}}^* + \frac{\partial\mathbf{F}}{\partial\mathbf{X}}|_{\mathbf{X}^*}(\mathbf{X}-\mathbf{X}^*) \tag{4}$$

Let $A=\frac{\partial\mathbf{F}}{\partial\mathbf{X}}|_{\mathbf{X}^*}$ and $\mathbf{x}=\mathbf{X}-\mathbf{X}^*$, then the Eq. (4) can be expressed as:

$$\dot{\mathbf{x}} = \mathbf{A}\mathbf{x} \tag{5}$$

The solution of the Eq. (5) can be written as:

$$\mathbf{x} = \mathbf{\Psi}(t,t_0)\mathbf{x}_0 \tag{6}$$

Where the $\mathbf{\Psi}(t,t_0)$is a state transition matrix. The correction of the initial state is denoted as $\mathbf{x}_0$. The observations at epoch t can be expressed as:

$$\mathbf{y} = \mathbf{H}\mathbf{x} + \varepsilon \tag{7}$$

Where ε and $\mathbf{D}$ denote the error and the covariance matrix of $\mathbf{y}$, respectively. The normal equation for the correction $\mathbf{x}$ can be derived by combining Eqs. (6) and (7), after employing the least square method.

$$\begin{cases}\left(\mathbf{\Psi}(t,t_0)^T\mathbf{H}^T\mathbf{P}\mathbf{H}\mathbf{\Psi}(t,t_0)\right)\mathbf{x} = \mathbf{\Psi}(t,t_0)^T\mathbf{H}^T\mathbf{P}\cdot\mathbf{y} \\ \mathbf{P} = \left(\sigma_0^2\mathbf{D}\right)^{-1}\end{cases} \tag{8}$$

The solvability of the normal Eq. (8) is contingent upon the invertibility of $\mathbf{\Psi}(t,t_0)^T\mathbf{H}^T\mathbf{P}\mathbf{H}\mathbf{\Psi}(t,t_0)$ on the left-hand side, which implies that $\mathbf{B}=\mathbf{H}\mathbf{\Psi}(t,t_0)$ must be a column-filling rank matrix, which means:

$$rank\left(\mathbf{H}\mathbf{\Psi}(t,t_0)\right) = k \tag{9}$$

Where k denotes the number of parameters to be estimated, it also equals the number of columns for $\mathbf{H}\mathbf{\Psi}(t,t_0)$.

Rank deficiency in autonomous navigation

When two satellites (designated as i and j) establish the ISL (as depicted below), the observation equation can be expressed as Eq. (1) (See Fig. 1).

If only the two-body problem is considered, according to the theory of POD, the matrix $\mathbf{B}=\mathbf{H}\mathbf{\Psi}(t,t_0)$ can be expressed as follows(Liu and Liu 2001):

$$\begin{aligned}\mathbf{B} &= \left(-\mathbf{e}_{ij}\cdot\frac{\partial\mathbf{r}_i}{\partial\mathbf{q}_i},\mathbf{e}_{ij}\cdot\frac{\partial\mathbf{r}_j}{\partial\mathbf{q}_j}\right) \\ &= \left[\begin{array}{cccccccccccc} B^i_a & B^i_e & B^i_{inc} & B^i_\Omega & B^i_\omega & B^i_M & B^j_a & B^j_e & B^j_{inc} & B^j_\Omega & B^j_\omega & B^j_M \end{array}\right]\end{aligned} \tag{10}$$

Where $\mathbf{r}_i$ and $\mathbf{r}_j$ denotes the position of satellite i and satellite j, respectively. $\mathbf{e}_{ij}$ denotes the direction from satellite i to

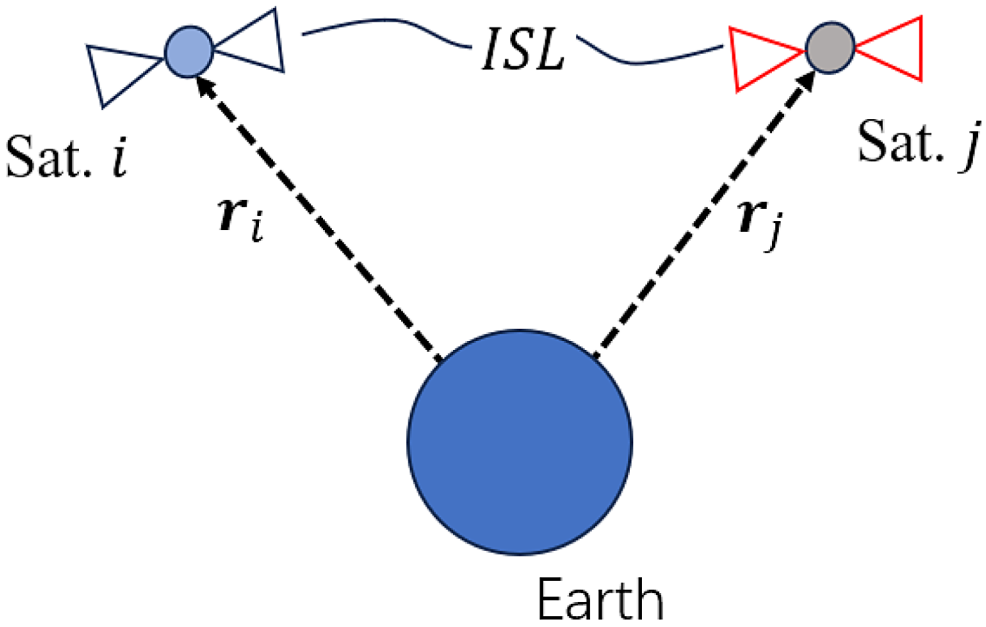

Fig. 1 Inter-satellite-link between satellite i and satellite j

satellite j. $\mathbf{q} = \begin{bmatrix} a & e & inc & \Omega & \omega & M \end{bmatrix}$ denotes the vector of orbit elements, it's also the parameter to be estimated. The coefficient B corresponds to each orbit element, with the lower corner indicating the respective orbit element and the upper corner denoting the corresponding satellite number.

According to the analysis by Liu and Li(Liu and Liu 2001), regardless of whether Satellite *i* or Satellite *j* is a LEO or GEO, the coefficients denoted as B^i_Ω and B^j_Ω corresponding to the right ascension of the ascending node in Eq. (10) are always opposite numbers. The inherent limitation renders it infeasible for the matrix $\mathbf{B}$ to satisfy the condition of column full rank, regardless of the number of observation epochs available. Consequently, the Eq. (8) becomes unsolvable, posing a significant challenge in autonomous navigation.

The gravitational asymmetric

The asymmetry of Earth's gravitational field, as argued by Hill and Born(Hill and Born 2007), is identified as the primary impediment for matrix $\mathbf{B}$ to satisfy the condition of column full rank. The orbital elements are all integral constants under spherically symmetric gravity, which can describe the characteristic of satellite motion influenced by the central body's gravitational force. When either the Earth or the Walker constellation rotates around the Earth's center, there is no change in force acting on the satellites. Consequently, both the shape and size of the orbits, as well as the relative positions between satellites, remain same, which have negligible impaction on ISL observations. This leads to an incapable determination of the absolute state of orbits and making ISL insensitive to absolute positioning in inertial space. Despite the inclusion of perturbations such as Earth's J2 and solar radiation pressure, their magnitudes remain insufficient to significantly enhance the observability of the equations.

If the central body's gravitational field is not spherical symmetry, and the extent of asymmetry significantly impacts the orbit of satellite, then during the rotation of two satellites around this central body, there will be a great variation in the ISL observation, thereby greatly enhancing the observability of the equations(Hesar et al. 2015). Hill(Hill 2007) also proposed that introducing a second celestial body to forming a three-body problem could amplify the asymmetry of the gravitational field in space and thus augment the observability of these equations.

The gravitational asymmetry coefficient α is employed by Hill to quantitatively measure the extent of gravitational asymmetry within the Earth-Moon system. Specifically, it represents the ratio between the magnitude of a spacecraft's third-body acceleration and the cumulative sum of all accelerations. The gravitational asymmetry coefficient α is expressed as follows:

$$a\left(x,y,z\right) = \frac{\left|\mathbf{a}_{3rd}\left(x,y,z\right)\right|}{\sum_{i=1}^{n}\left|\mathbf{a}_i\left(x,y,z\right)\right|} \tag{11}$$

Where $a_i(x,y,z)$ denotes the satellite's acceleration affected by perturbation force $i(i=1\cdots n)$, and $a_{3rd}(x,y,z)$ denotes the acceleration affected by the gravitational force of the 3rd body. In cislunar space, the Moon is treated as a 3rd body when the satellite is close to the Earth due to Earth's stronger gravitational force; conversely, the Earth is treated as a 3rd body when the satellite is closing to the Moon. Figure 2

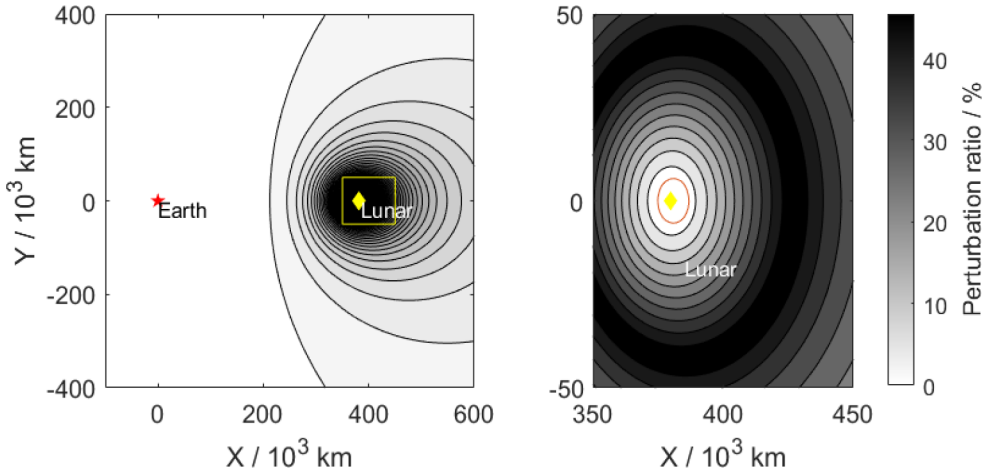

Fig. 2 The gravitational asymmetry coefficient in Cislunar space, and the right figure shows detail in moon space

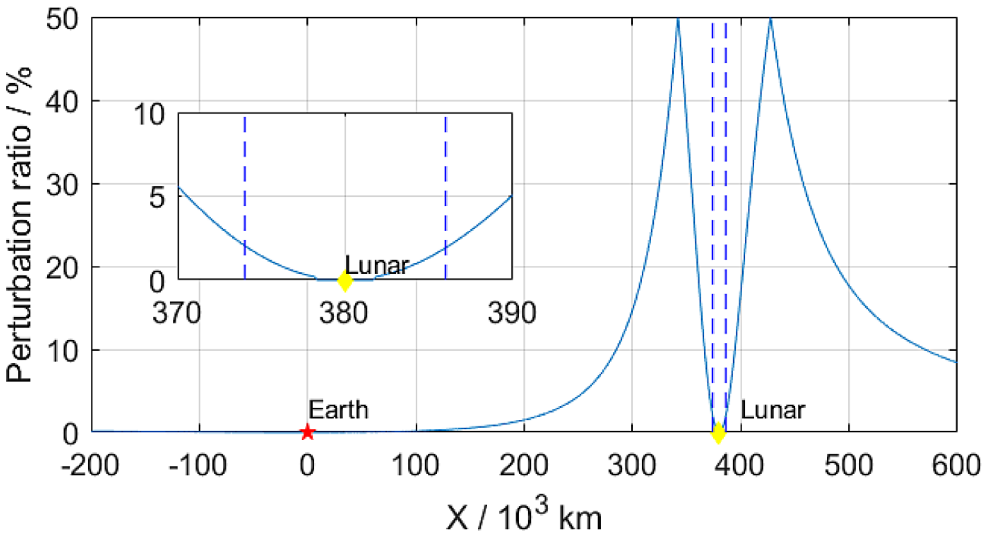

Fig. 3 The gravitational asymmetry coefficient slice on the earth-moon line

shows the gravitational asymmetry coefficient α in the X-Y plane of the Earth-Moon rotating system.

The proximity of Earth's gravity and lunar gravity are represented by the darker color in Fig. 2. The α value of the three-body gravitational field in this region directly influences the feasibility and accuracy of autonomous navigation when satellites establish ISL with other orbits. The data has been segmented at Y = 0 to conduct a more comprehensive analysis of the evolving asymmetry trend, as depicting in the Fig. 3.

According to Fig. 3, the asymmetry coefficient between the Earth and the Moon exhibits a trend of initially increase and then decrease. The current engineering tasks for lunar exploration are primarily conducted near the Moon. For example, the Chang'e-1 mission operated at a height of only 200 km in a circular orbit(Chen et al. 2011), while the Chang'e-2 mission maintained an orbit altitude of just 100 km(Chen et al. 2012). Within these regions near the Moon, particularly within a distance of 6000 km from its surface, all asymmetry coefficients have been calculated to be less than 5%. But the possibility of the satellites in this region for inter-satellite autonomous navigation is still exist, when there is a satellite being close to the Earth while another being close to the Moon, the overall gravitational field asymmetry extent within this system becomes significantly pronounced. Certainly, it should be noted that solely considering gravitational asymmetry does not provide a comprehensive understanding of the issue. Nevertheless, the research conducted on inter-satellite autonomous navigation based on this scenario is not too much.

Building upon previous research by Liu and Liu(Liu and Liu 2001), this paper further substantiates the viability of autonomous navigation based on ISL under such unique circumstances.

The feasibility analysis of a special scenario

At a given epoch *t*, the position vector of the Moon relative to Earth is denoted as $\mathbf{r}_m$, and its velocity vector is $\mathbf{v}_m$. The position and velocity vectors of Earth's satellite *i* relative

to Earth in the Earth-centered inertial system(ECI) are represented by $\mathbf{r}_i$ and $\mathbf{v}_i$ respectively, with their orbital elements being $\mathbf{q}_i = \left[\ a_i \ \ e_i \ \ inc_i \ \ \Omega_i \ \ \omega_i \ \ M_i\ \right]^T$. Additionally, a Moon's satellite *i* has a sufficiently low altitude and negligible influence from Earth's gravity, its position and velocity vectors in the lunar inertial system can be denoted as $\mathbf{r}_j$ and $\mathbf{v}_j$ respectively, while its orbital elements relative to the Moon are referred to as $\mathbf{q}_j = \left[\ a_j \ \ e_j \ \ inc_j \ \ \Omega_j \ \ \omega_j \ \ M_j\ \right]^T$. Also, we simulate an ISL scenario between the Earth satellite *i* and Moon satellite *j*, as shown in the Fig. 4.

The deduction results presented by Liu and Li(Liu and Liu 2001) showed that the partial derivative of the satellite position vector for the right ascension of ascending node Ω could be expressed as follows:

$$\begin{cases} \frac{\partial \mathbf{r}_i}{\partial \Omega} = \left(\ -y_i \ \ x_i \ \ 0\ \right)^T \\ \frac{\partial \mathbf{r}_j}{\partial \Omega} = \left(\ -y_j \ \ x_j \ \ 0\ \right)^T \end{cases} \tag{12}$$

Also, B_Ω^i and B_Ω^j in Eq. (10) can be expressed as:

$$\begin{cases} B_\Omega^i = -\mathbf{e}_{ij} \cdot \frac{\partial \mathbf{r}_i}{\partial \Omega} \\ B_\Omega^j = \mathbf{e}_{ij} \cdot \frac{\partial \mathbf{r}_j}{\partial \Omega} \end{cases} \tag{13}$$

Where $\mathbf{e}_{ij}$ denotes the direction vector from the position of satellite *i* to the position of satellite *j*. Assuming the effects of relativity are neglected, and basing on the known position and velocity of the moon, $\mathbf{e}_{ij}$ in the expression (13) can be written as below when the J2000.0 Earth-centered inertial coordinate system is adopted as the reference frame.

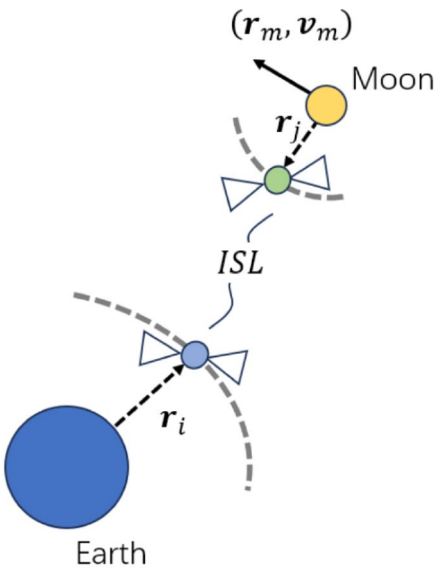

Fig. 4 Inter-satellite-link between Earth-satellite j and Moon-satellite j

$$\mathbf{e}_{ij} = \frac{\mathbf{r}_j + \mathbf{r}_m - \mathbf{r}_i}{|\mathbf{r}_j + \mathbf{r}_m - \mathbf{r}_i|} \tag{14}$$

After combining (12), (13) and (14):

$$\begin{cases} B_\Omega^i = -\frac{1}{L_{ij}} \cdot (x_i y_j - x_j y_i - x_m y_j + x_j y_m) \\ B_\Omega^j = \frac{1}{L_{ij}} \cdot (x_i y_j - x_j y_i - x_m y_i + x_i y_m) \end{cases} \tag{15}$$

The relationship between B_Ω^i and B_Ω^j no longer exhibits opposition, and the columns associated with the matrix $\mathbf{B}$ in the Eq. (10) are now characterized by linear independence, thereby the solvability conditions for autonomous navigation based on ISL are established.

It is imperative to note that Eq. (15) remains valid exclusively when satellite *i* and satellite *j* adhere to predetermined Keplerian orbits, influenced by the gravitational forces exerted by their respective central celestial bodies. In other words, once the position and velocity of the moon are determined, it can serve as an inertial reference for satellite *i* and satellite *j* based on its gravitational force.

Based on the aforementioned theory, we propose deploying a spacecraft in the cislunar space that can be captured by lunar gravity and connected to the GNSS constellation in near-Earth space through ISL. This approach can leverage the gravitational influence of the Moon on this spacecraft to provide a directional reference for the GNSS constellation during autonomous navigation periods.

In this paper, simulation analysis will be conducted to evaluate autonomous navigation based on ISL under this scenario. Considering the significance of ISL, we will focus on analyzing the correction performance of orbit elements for GNSS constellations.

Settings for simulation and precise orbit determination

(1) Constellation type: We employ a Walker constellation of 24 MEO satellites to represent the GNSS constellation, which is distributed across 3 orbital planes with PRN ranging from G01 to G24. Additionally, a satellite named LunarSat is deployed near the moon with a PRN G25. The orbital information of 24 GNSS satellites and LunarSat is listed in the tables below (See Table 1 and 2).

(2) Initial epoch: 2020-06-05T00:00:00 (GPST).

(4) Number of arcs: 60. Length of each arc: 3 days. Overlap between adjacent arcs: 1 day.

(3) Simulation duration: 120 days.

(4) Number of arcs: 60. Length of each arc: 3 days. Overlap between adjacent arcs: 1 day.

(5) Settings for observation, orbit integral, and POD:

Table 1 Information of orbital plane of GNSS satellites

Number	Semi-major axis	Orbital Period	Eccentricity	Inclination	Node	PRN
1	27900.0 km	12.88 h	0.000001	55°	120°	1~8
2					240°	9~16
3					0°	17~24

Table 2 Orbital elements of LunarSat in the Lunar inertial system

	Value
Semi-major axis	6007.7 km
Orbital Period	11.6 h
Eccentricity	0.149
Inclination	24°

Table 3 Settings for ISL simulation, orbital integration, and POD

Reference frame, perturbation force, simulation parameters, and solving strategy	Description
Reference System	J2000.0
Precession/Nutation Model	IAU 2006/IAU 2000R06(Petit and Luzum 2010)
Lunar Rotation Model	IAU 1980(Davies et al. 1980)
Earth rotation parameters	EOP from IERS
Earth gravity	EIGEN-GL04C(70*70)(Förste et al. 2008)
Moon gravity	GRGM900c(4*4)(Lemoine et al. 2014)
N body	DE405
Solar radiation pressure	GNSS: ECOM5(Guo 2014) LunarSat: Spherical Model
General Relativity	IERS Conventions 2010(Petit and Luzum 2010)
Earth Tides	IERS Conventions 2010(Petit and Luzum 2010)
Ranging accuracy in simulation	GNSS-GNSS: 1 cm; GNSS-LunarSat: 1 m
Data sampling interval	300 s
Radius: of ISL payload's pointing range	45 degrees
Parameter estimation methods	least squares batch processing
Outlier Elimination Method	3_{σ} criterion
Integrator	Cowell integrator
Estimated parameters	GNSS: orbit elements and 5 parameters of ECOM5 for each arc LunarSat: orbit elements and a solar pressure factor for each arc

Based on previous project experience, we set a ranging accuracy of 1 cm between GNSS satellites and 1 m between GNSS satellites and LunarSat. Considering the requirement for reciprocal pointing in establishing inter-satellite communication links, we limit the radius of the ISL payload's pointing range to 45 degrees.

We adopt the J2000.0 inertial coordinate system as our reference frame and utilize the precession/nutation models recommended by the IERS Conventions 2010 during the simulation and POD. As this simulation primarily validates the effectiveness of the LunarSat in mitigating GNSS constellation drift, without considering the error caused by long-term prediction of Earth Orientation Parameters (EOP). Instead, we directly adopt the EOP product released by IERS.

We employ the JGM70*70 Earth gravity field model for GNSS satellites and incorporate the ECOM-5 to model the solar radiation pressure. Regarding LunarSat, we apply the GRGM900c(4*4) model for non-spherical lunar gravity while considering only one solar radiation pressure coefficient for each arc. Additionally, general relativity effects and Earth tidal perturbations are incorporated using models recommended by the IERS conventions 2010 for each satellite. In terms of parameter estimation, a least squares batch processing method is employed for POD. For each GNSS satellite, initial epoch orbital elements are estimated for each arc segment along with solving for the five parameters of the ECOM model. Similarly, in the case of LunarSat, its orbital elements are estimated while also solving for solar radiation pressure coefficients in each arc segment. Other settings are listed in the table below (See Table 3).

(6) Establishment of ISL: We establish ISL for 24 GNSS satellites, adhering to the ISL of BDS shown in the Fig. 5(G12 is used as an example in this figure)(Xie 2020). Every GNSS satellite establishes ISLs with two adjacent satellites in the same plane, and also with two neighboring satellites in different planes. Meanwhile, to obtain as much observation as possible, considering the requirement for reciprocal pointing in establishing inter-satellite communication links, we allow the links to be established as long as two satellites within the antenna pointing range of each other (We assume that the ISL antenna pointing is always in the same direction with the vector extending from the central body to its respective position). In this scenario, every GNSS satellite can acquire a maximum of four ISL observations in an epoch, and one observation from the GNSS-LunarSat ISL (See Fig. 6).

(7) Description of Experiment Plan:

To validate the efficacy of ISL between GNSS and LunarSat in POD, this study has devised two sets of simulation experiments for comparative analysis. The specific details are presented in the table provided (See Table 4).

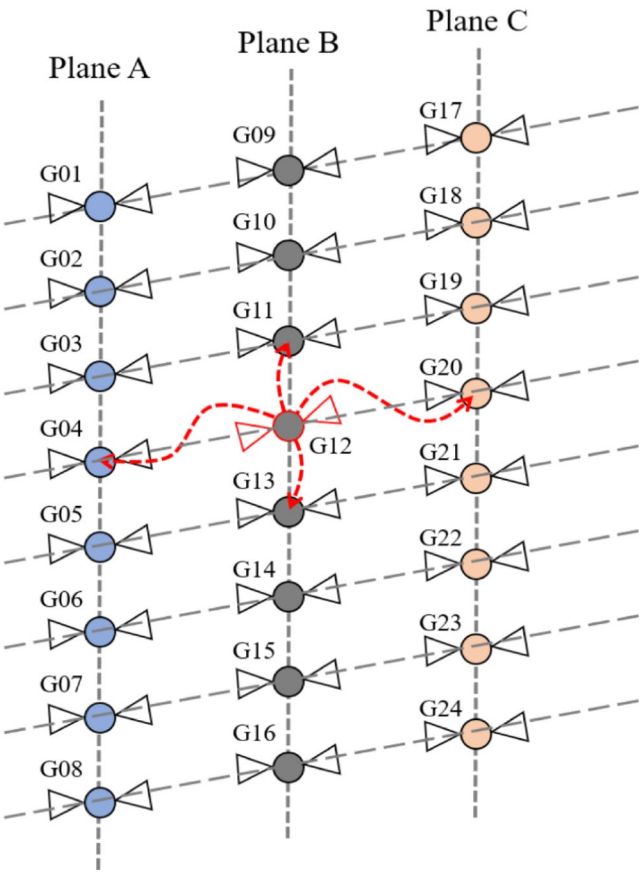

Fig. 5 Phase Diagram of the GNSS Constellation and its establishment process of ISL

Table 4 Description of two sets of simulation experiments

	Name	Description
Plan A	S (GNSS only)	ISLs are established by only GNSS satellites.
Plan B	SL (GNSS + LunarSat)	ISLs are established by GNSS satellites, and also between GNSS and LunarSat.

Result and analysis

Status of observations

We collect a total of 1,393,702 observations during the 120-day simulation period. Among them, the proportion of visible epochs between GNSS and LunarSat is determined to be 16.37% of the total epochs. There is a total of 11,302 GNSS-LunarSat observations, accounting for 0.81% of all observations. Furthermore, as illustrated in Fig. 7 (a) and (b), LunarSat consistently receives observational data while positions in the region between Earth and the Moon, with its track of sub-satellite points evenly distributed on the lunar-facing side.

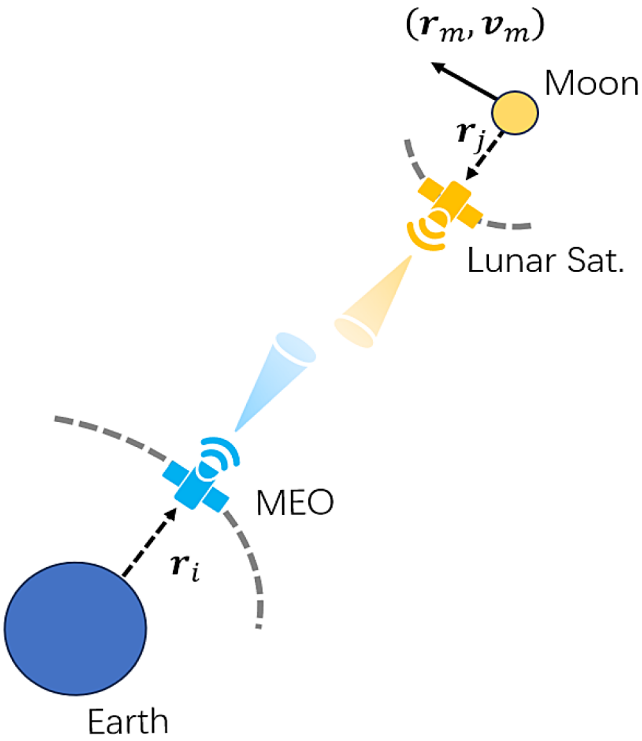

Fig. 6 Establishment process of ISL between GNSS and LunarSat

Analysis of GNSS results

The residuals' root mean square (RMS) is a crucial metric for assessing the precision of POD. We have counted the residuals' RMS of the ISLs between GNSS satellites for all 59 arcs in this simulation, as shown in the Fig. 8.

The autonomous navigation network solution based on the ISL of GNSS satellites demonstrates an average residual RMS of 1.22 cm (S scheme), while the combined ISL of GNSS and LunarSat demonstrate an average RMS of 1.42 cm (SL scheme), as shown in the Fig. 8.

The difference in the mean-RMS between S and SL schemes is not statistically significant, with both values closely aligned with the observation errors specified in the simulation. Considering the establishment method of ISL previously described, this implies that the relative positions among GNSS satellites are effectively maintained under both schemes, which indicates few changes in the size and shape of the GNSS constellation.

However, after comparing with the simulated orbit (truth values), we found a huge difference in the accuracy of the POD results between S and SL schemes, as shown in the Fig. 9, even though their residual RMSs are very similar. The average RMS of the POD result of S schemes is 408.56 m compared to 7.78 m for the SL scheme, and there is a 98% improvement in the accuracy of the SL scheme.

The SL scheme demonstrates superior accuracy primarily in the tangential (T) and normal (N) directions of the orbit,

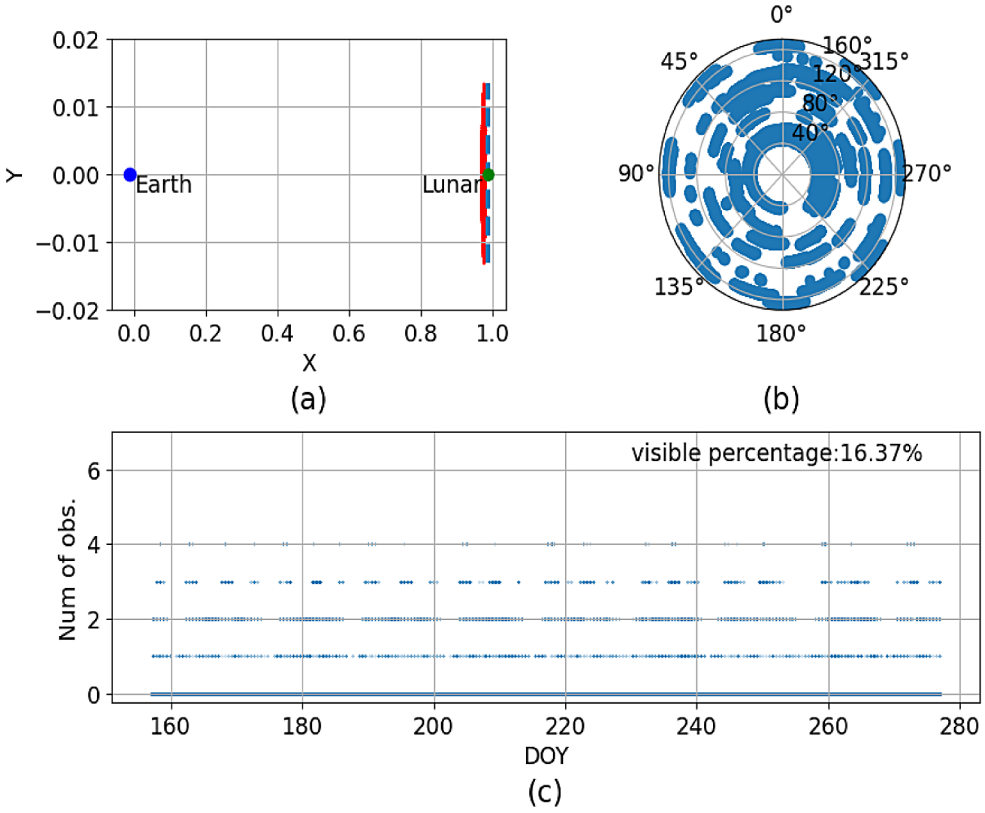

Fig. 7 The ISL observation status of MEO-LunarSat is depicted as follows: (**a**) Illustration of the distribution of LunarSat in the Earth-Moon Conjunction Coordinate System at the time of observation, with the coordinate origin being the center of mass of the Earth-Moon system. The X-axis represents the line connecting the Earth and the Moon, while the Y-axis is parallel to this line within a plane containing it. All axes are measured in units corresponding to the distance between the Earth and the Moon. (**b**) Track of subsatellite point for LunarSat on the lunar hemisphere facing Earth at each observation epoch. (**c**) Quantities of MEO-LunarSat ISL observations at each epoch

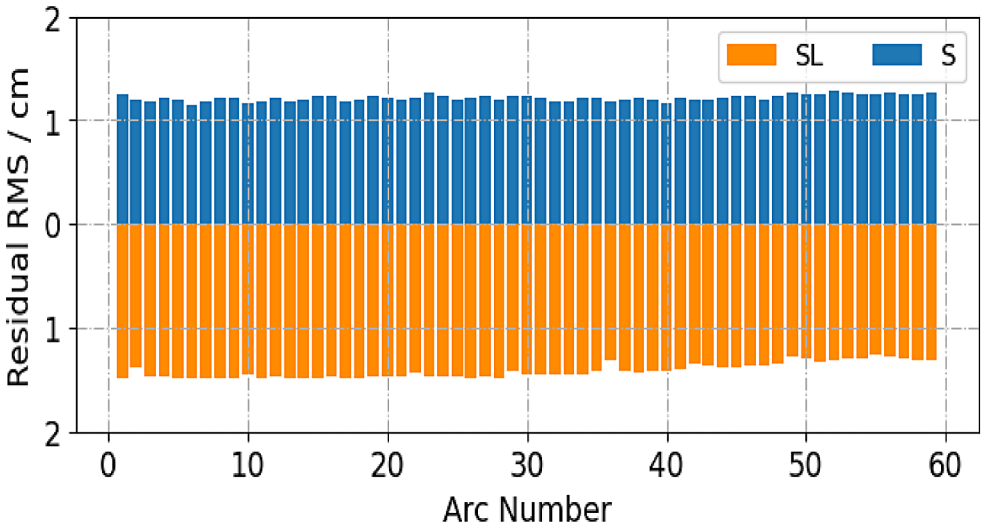

Fig. 8 The residual RMS of both the S scheme and SL scheme in each arc

while there are few differences between the S scheme and SL scheme in terms of radial(R) accuracy, with both better than 5 cm, as shown in the Fig. 10; Table 5. This indicates that ISL possesses the capability to accurately determine the size and shape of orbits, even in the absence of LunarSat's integration into the ISL net.

The T and N directions primarily provide information about the position and orientation of a satellite in an inertial system. As a result, the result of scheme S exhibits a noticeable overall rotation of the constellation. However, with the inclusion of LunarSat in ISL, situated within lunar orbit, there has been a significant enhancement in the orbital accuracy of each GNSS satellite along both the T and N directions by 89.6% and 98.6%, respectively, and this improvement signifies a suppression of overall constellation rotation.

We have also noticed some periodic significant errors under the SL scheme, with magnitudes approaching those of the S scheme. We propose that LunarSat's observations play a pivotal role in contributing to this phenomenon, thus

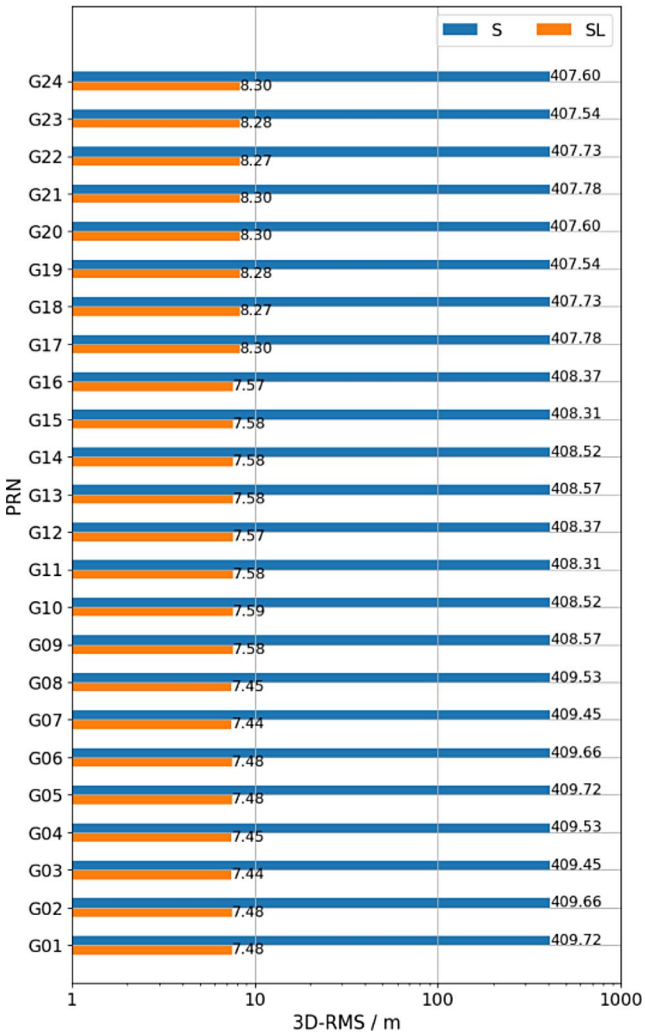

Fig. 9 The 3D-RMS of each GNSS satellite under scheme S and SL compared with the simulated orbit (truth values)

necessitating further analysis and discussion in the subsequent section.

Based on the research by Liu and Liu(Liu and Liu 2001), it is advisable to analyze the inhibitory effect of the SL scheme on constellation rotation by analyzing orbital elements. Taking G02, G12, and G22 as examples, we complete the analysis of the orbital element that depicts orbital orientation (inclination angle, right ascension of ascending node, argument of perigee, and mean anomaly), as shown in the Fig. 11; Table 6.

As shown in Fig. 11, all the orbital parameters that can describe the orbital orientation have a huge estimation error under the S scheme, with an average RMS of 0.363 degrees for the inclination angle, 4.221 degrees for the right ascension of ascending node, and 0.361 degrees for the sum of the argument of perigee and mean anomaly. The error in the right ascension of the ascending node is significantly larger than that of other orbital elements, and due to the linear correlation among the coefficients of the aforementioned equations, the error does not exhibit a clear temporal evolution either. Despite employing relatively comprehensive dynamic modeling for POD, we are still unable to rectify the ill-conditioned nature of these equations, resulting in an inaccurate estimation of the right ascension of the ascending node in scheme S.

In the SL scheme, LunarSat, as a lunar satellite, is subject to the gravitational constraints of the moon. Consequently, it serves as a spatial anchor point guiding the autonomous navigation of the GNSS constellation in ISL. The inclusion of LunarSat has resulted in a significant enhancement in the accuracy of all orbital parameter determinations. Notably, there has been an approximate 89% improvement in the inclination angle, around 99% improvement in the right ascension of the ascending node, and approximately 89% improvement in the sum of the argument of perigee and mean anomaly.

The fact that the ISL observation of GNSS-LunarSat only constitutes 0.81% of all observations. Nobatly, such a minute amount of observational data can yield such a substantial enhancement in accuracy, thereby indicating the profound impact of employing LunarSat as a spatial anchor point on suppressing the overall drift within the autonomous navigation based on ISL.

Analysis of LunarSat results

In the analysis above, we have found consistent periodic significant errors in the SL scheme. We have postulated that this phenomenon could be attributed to certain limitations in the observation data of LunarSat, such as the lack of observation during some specific epochs. Consequently, we have analyzed the observation number and the orbit estimation accuracy of LunarSat, as shown in the Fig. 12.

Compared to GNSS satellites, LunarSat exhibits significantly lower orbit determination accuracy with an average 3D-RMS of 79.04 m. This discrepancy can be attributed to both its substantial ranging error and pool observation geometry, as well as the limited availability of observational data. Particularly in Fig. 12 (a), most arcs are fewer than 200 observations, and some even approach to zero. As the number of observations decreases, the orbit determination accuracy of LunarSat rapidly deteriorates to a magnitude on the order of hundreds of meters. Consequently, this decrease in precision also affects GNSS satellites as it introduces uncertainties in parameters related to estimating their orbit orientation and eventually leads to noticeable drift within the GNSS constellation.

The limited number of observations is attributed to the substantial distance between MEO and LunarSat, which presents challenges in aligning the antenna and results in

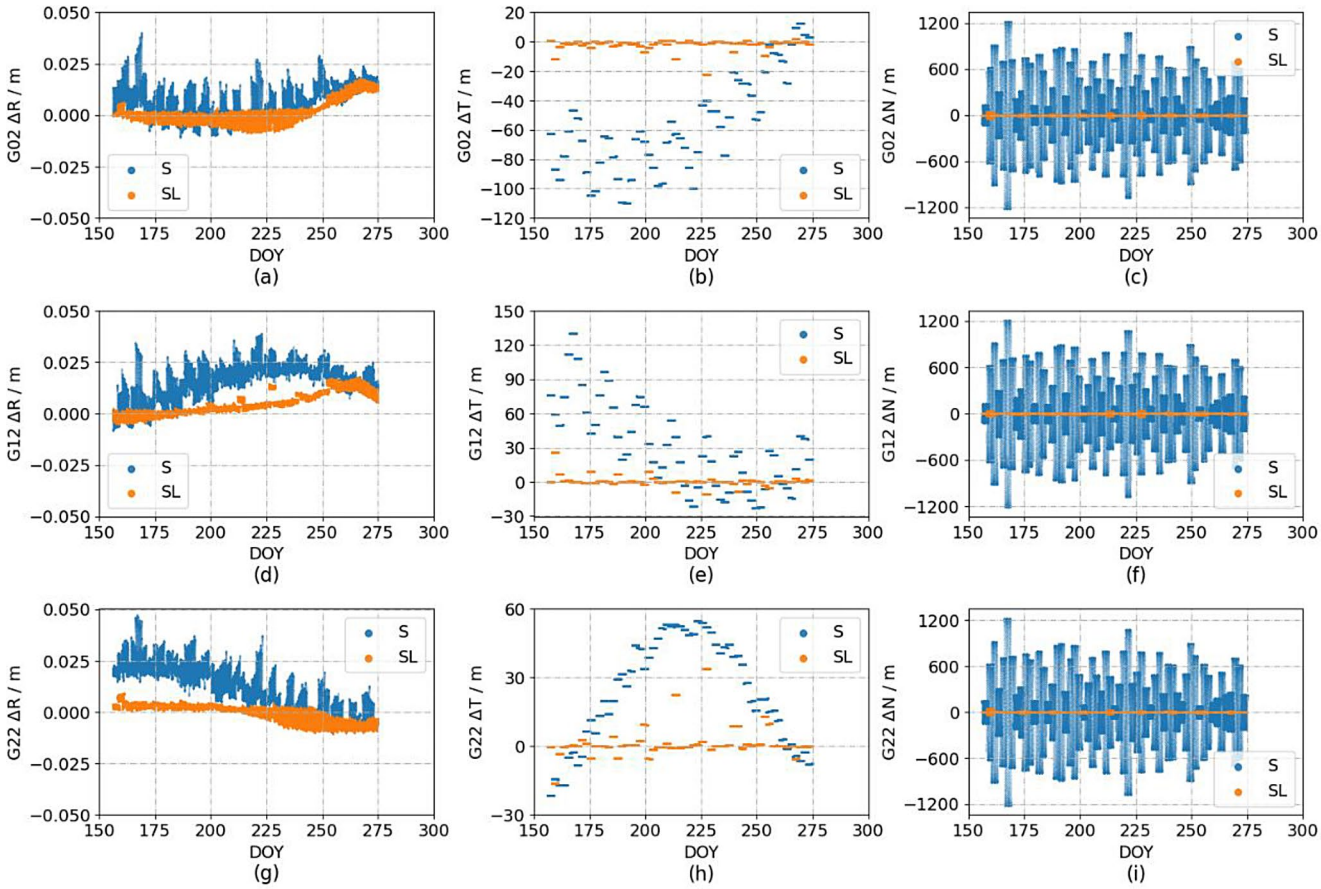

Fig. 10 The POD result error of G02, G12, and G22 in R, T, and N direction of each epoch under scheme S and SL compared with the simulated orbit (truth values). (**a**)-(**c**) The error of G02 in the R, T, and N direction of each epoch; (**d**)-(**f**) The error of G12 in the R, T, and N direction of each epoch; (**g**)-(**i**) The error of G22 in R, T, and N direction of each epoch

Table 5 The RMS of G02, G12, and G22 in R, T, and N direction under scheme S and SL compared with the simulated orbit (truth values)

PRN	Scheme	*R*-RMS / m	T-RMS / m	*N*-RMS / m
G02	S	0.010	65.133	404.448
	SL	0.006	4.259	6.154
G12	S	0.018	48.587	405.472
	SL	0.007	4.656	5.975
G22	S	0.016	33.028	406.395
	SL	0.004	6.641	4.933

a relatively low probability of successful communication. Moreover, this simulation only utilizes one lunar satellite and also impose constraints on establishing ISL conditions. Consequently, when the orbital plane of LunarSat is perpendicular to the earth-moon direction, it becomes difficult for LunarSat to establish contact with GNSS satellites, thereby reducing the number of relevant observations.

We need to note that this simulation is based on the existing ISL technology for GNSS, with easier establishment of communication links during implementation. A forthcoming technical consideration emerges: how to optimize the observation scheme to maximize GNSS-LunarSat's observation accuracy while minimizing costs.

Conclusion

In essence, ISL can't establish a stable connection with inertial space, both at the observation and dynamic modeling levels, the primary cause of the overall drift in the autonomous navigation. Consequently, while accurate estimation of the size and shape of the constellation can be achieved within the network solution of autonomous navigation, there is a significant error in estimating orbit orientation parameters. This paper proposes an inter-satellite link networking method that incorporates space anchor satellites utilizing lunar gravity as a directional benchmark to enhance the solution ability of orbit parameters across the entire GNSS constellation. The feasibility of this approach in mitigating constellation drift is verified through theoretical analysis and simulation experiments, and the following useful conclusions are obtained:

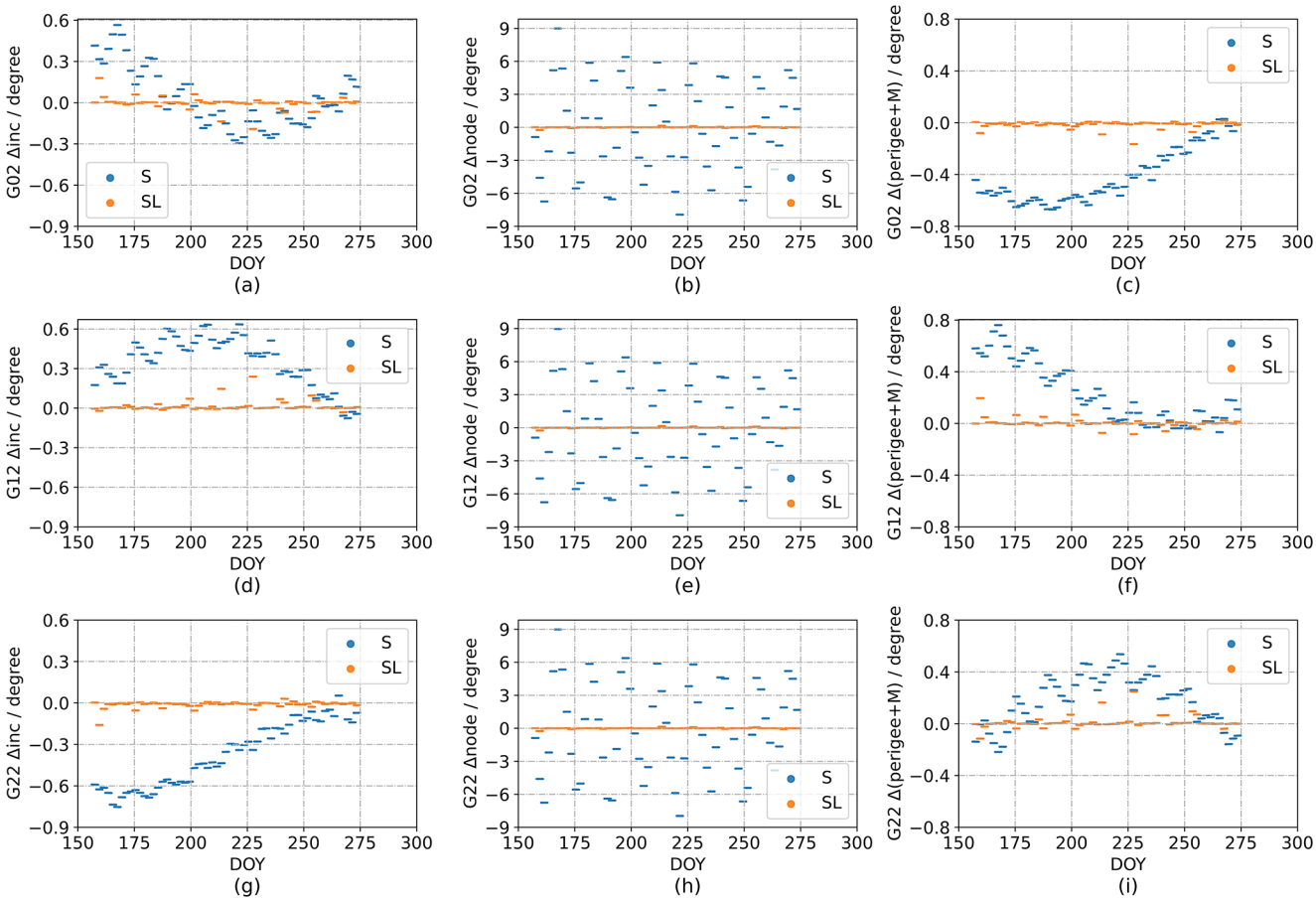

Fig. 11 The orbital elements estimation error(for only inclination angle, right ascension of ascending node, and the sum of the argument of perigee and mean anomaly) of G02, G12, and G22 of each epoch under scheme S and SL compared with the simulated orbit (truth values). (**a**)-(**c**) The error of G02 of each epoch; (**d**)-(**f**) The error of G12 of each epoch; (**g**)-(**i**) The error of G22 of each epoch

Table 6 The RMS of orbital elements (for only inclination angle, right ascension of ascending node, and the sum of the argument of perigee and mean anomaly) of G02, G12, and G22 under scheme S and SL compared with the simulated orbit (truth values)

PRN	Scheme	RMS / degree		
		Inc	Node	Perigee+M
G02	S	0.218	4.222	0.463
	SL	0.045	0.045	0.031
G12	S	0.392	4.216	0.329
	SL	0.043	0.046	0.035
G22	S	0.440	4.225	0.264
	SL	0.027	0.044	0.048

1. According to the proposed approach, the inclusion of LunarSat, a lunar satellite, in the ISL significantly enhances the accuracy of autonomous navigation network solutions by over 97%. This improvement is primarily observed in both the orbit T direction and N direction with an impressive increase of 89.6% and 98.6%, respectively.
2. The autonomous navigation based on the ISL of GNSS+LunarSat leverages the moon's gravity to establish a spatial reference for the entire constellation. Through the analysis of the orbital elements of GNSS satellites, we find that this approach significantly enhances orbit orientation estimation accuracy. Specifically, we achieve an improvement of approximately 89% in the accuracy of the inclination angle, around 99% in the right ascension of ascending node, and about 89% in the sum of the argument of perigee and the mean anomaly.
3. The limited number of inter-satellite measurements of GNSS-LunarSat remains a primary constraint on the accuracy of results obtained through this method. In such cases, establishing a persistent connection between GNSS and LunarSat proves challenging, leading to an inherent overall drift phenomenon within the constellation when observations are scarce. Consequently, it becomes imperative to explore more efficient observation methods that can maximize data collection while ensuring high-precision measurements.

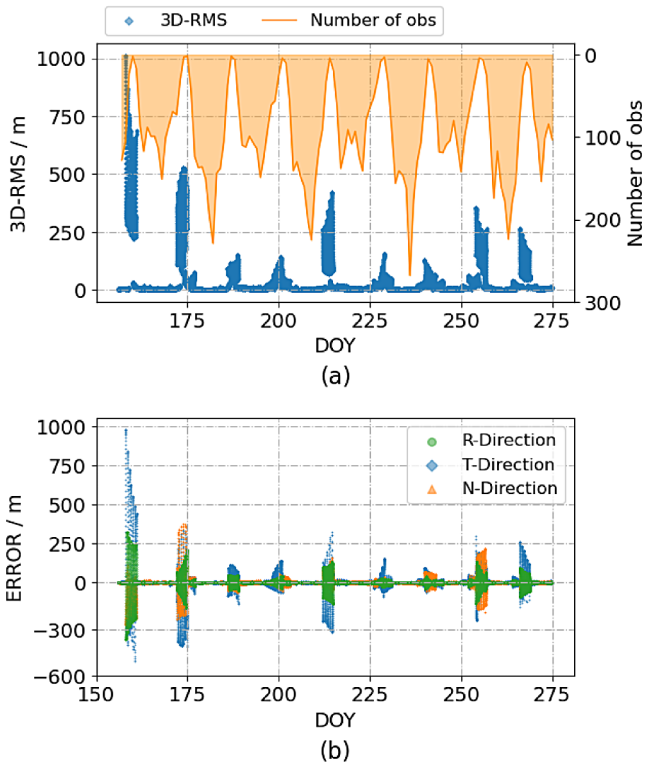

Fig. 12 The POD result error of LunarSat of each epoch compared with the simulated orbit (truth values). (**a**) The blue line indicates the 3D-RMS of LunarSat of each epoch, while the orange line indicates the number of GNSS-LunarSat ISL observations; (**b**) The error of LunarSat in R, T, and N direction of each epoch

Meanwhile, the simulation in this paper primarily relies on the ground server for calculations using the batch processing method. However, due to limitations in the computing capacity and storage space of the onboard processor, this study mainly focuses on validating the feasibility and effectiveness of the proposed approach.

Acknowledgements We appreciate the reviewers and editors' valuable comment to improve the paper quality.

Author contributions P.L. and Y.S. wrote the main manuscript text; P.L., Y.S. and J.Y. designed and implemented simulation experiments; J.Y. revised the manuscript; X.H. and C.T. supplied guidance on relevant knowledge and the simulation software; K.L. provided software guidance to P.L.;Q.W. revised the format of the paper, and also made grammar and content modifications.All authors reviewed the manuscript.

Funding Not applicable.

Data availability No datasets were generated or analysed during the current study.

Declarations

Ethics approval and consent to participate We declare that this manuscript described a complete original work, and the results/data/figures in this manuscript have not been published elsewhere, nor are they under consideration (from you or one of your Contributing Authors) by another publisher.

Consent for publication We declare that all authors agreed with the content and that all gave explicit consent to publication.

Competing interests The authors declare no competing interests.

References

Chen M, Tang G, Cao J, Zhang Y (2011) Precision Orbit determination of CE-1 Lunar Satellite. Geomat Inf Sci Wuhan Univ 36(2):212–217. https://doi.org/10.13203/j.whugis2011.02.016

Chen M, Zhang Y, Cao J, Li X, Tang G, Wang J, Duan J, Xie J, Tong B (2012) Orbit determination and tracking technology of CE-2 satellite. Chin Sci Bull 57(9):689–696. https://doi.org/10.1360/972011-818

Davies ME, Abalakin VK, Cross CA, Duncombe RL, Masursky H, Morando B, Owen TC, Seidelmann PK, Sinclair AT, Wilkins GA, Tjuflin YS (1980) Report of the IAU Working Group on Cartographic Coordinates and rotational elements of the planets and satellites. Celest Mech 22(3):205–230. https://doi.org/10.1007/BF01229508

Förste C, Schmidt R, Stubenvoll R, Flechtner F, Meyer U, König R, Neumayer H Biancale R (2008) The GFZ/GRGS satellite and combined gravity field models EIGEN-GL04S1 and EIGEN-GL04C

Guo J (2014) The impacts of attitude, solar radiation and function model on precise orbit determination for GNSS satellites. PHD, Wuhan University

Hesar S, Parker J, Mcmahon J, Born G (2015) Small body gravity field estimation using LIAISON supplemented optical navigation. In: AAS GN&C Conference

Hill KA (2007) Autonomous Navigation in Libration Point Orbits. PHD, University of Colorado

Hill K, Born GH (2007) Autonomous Interplanetary Orbit determination using Satellite-to-Satellite Tracking. J Guid Control Dyn 30(3):679–686. https://doi.org/10.2514/1.24574

Huang Y, Yang P, Chen Y, Li P, Zhou S, Tang C, Hu X (2022) Orbit determination of a cislunar space probe using Inter-satellite Link data. Sci Sin Phys Mech Astron 53(2). https://doi.org/10.1360/SSPMA-2022-0176

Lemoine FG, Goossens S, Sabaka TJ, Nicholas JB, Mazarico E, Rowlands DD, Loomis BD, Chinn DS, Neumann GA, Smith DE, Zuber MT (2014) GRGM900C: a degree 900 lunar gravity model from GRAIL primary and extended mission data. Geophys Res Lett 41(10):3382–3389. https://doi.org/10.1002/2014GL060027

Li X, Hu X, Guo R, Tang C, Liu S, Xin J, Guo J, Tian Y, Yang Y, Yang J, Zhao X (2023) Precise orbit determination for BDS-3 GEO satellites enhanced by intersatellite links. GPS Solut 27(1):8. https://doi.org/10.1007/s10291-022-01330-3

Liu Y-C, Liu L (2001) Orbit determination using Satellite-to-Satellite Tracking Data. Chin J Astron Astrophys 1(3):281–286. https://doi.org/10.1088/1009-9271/1/3/281

Markley F (1984) Autonomous navigation using landmark and intersatellite data. In: Astrodynamics Conference. American Institute of Aeronautics and Astronautics, Seattle,WA,U.S.A

Parker J, Anderson R, Born G, Fujimoto K, Leonard J, McGranaghan R (2012) Navigation Between Geosynchronous and Lunar L1 Orbiters. In: AIAA/AAS Astrodynamics Specialist Conference. American Institute of Aeronautics and Astronautics, Minneapolis, Minnesota

Petit G, Luzum B (2010) IERS conventions (2010). Tech Rep DTIC Doc 36:180

Psiaki ML (1999) Autonomous Orbit determination for two spacecraft from relative position measurements. J Guid Control Dyn 22(2):305–312. https://doi.org/10.2514/2.4379

Psiaki M (2007) Absolute Orbit and Gravity Determination Using Relative Position Measurements Between Two Satellites. In: AIAA Guidance, Navigation and Control Conference and Exhibit. American Institute of Aeronautics and Astronautics, Hilton Head, South Carolina

Tang C, Hu X, Zhou S, Pan J, Guo R, Hu G, Zhu L, Li X, Wu S, Wang Y (2017) Centralized autonomous orbit determination of Beidou navigation satellites with inter-satellite link measurements: preliminary results. Sci Sin Phys Mech Astron 47(2):029501. https://doi.org/10.1360/SSPMA2016-00355

Tang C, Hu X, Zhou S, Liu L, Pan J, Chen L, Guo R, Zhu L, Hu G, Li X, He F, Chang Z (2018) Initial results of centralized autonomous orbit determination of the new-generation BDS satellites with inter-satellite link measurements. J Geod 92(10):1155–1169. https://doi.org/10.1007/s00190-018-1113-7

Tang C, Hu X, Chen J, Liu L, Zhou S, Guo R, Li X, He F, Liu J, Yang J (2022) Orbit determination, clock estimation and performance evaluation of BDS-3 PPP-B2b service. J Geod 96(9):60. https://doi.org/10.1007/s00190-022-01642-9

Xie X (2020) Precise orbit and clock determination for BDS-3 satellites using inter-satellite link observations. PHD, Wuhan University

Xie X, Geng T, Zhao Q, Cai H, Zhang F, Wang X, Meng Y (2019) Precise orbit determination for BDS-3 satellites using satellite-ground and inter-satellite link observations. GPS Solut 23(2):40. https://doi.org/10.1007/s10291-019-0823-5

Yang J, Hu X, Zhou W, Zhou S, Tang C, Song Y, Liu L, Yang Y, Tian Q, Liu J, Liu Y, Xing N, Ma Y (2023a) Relativistic effects in BDS-3 high-accuracy intersatellite time synchronization. Adv Space Res:S 0273117723001643. https://doi.org/10.1016/j.asr.2023.02.036

Yang J, Tang C, Hu X, Zhou S, Liu L, Song Y, Yang Y, Guo R, Liu S, Pan J (2023b) Centimeter-level clock synchronization and space-borne timescale generation for BDS-3 using inter-satellite link measurements. J Geod 97(8):77. https://doi.org/10.1007/s00190-023-01765-7

Zhang Y (2005) Study on autonomous navigation of constellation using inter-satellite measurement. PHD, National University of Defense Technology

Zhang L, Xu B (2015) Navigation Performance of the Libration Point Satellite Navigation System in Cislunar Space. J Navig 68(2):367–382. https://doi.org/10.1017/S0373463314000617

Peng Luo is currently a doctoral degree candidate at the Shanghai Astronomical Observatory, Chinese Academy of Sciences. His main research interests are Precise Orbit Determination for spacecraft and its applications.

Ye-Zhi Song is a senior engineer at Shanghai Astronomical Observatory, Chinese Academy of Sciences. He received his Ph.D. degree from University of Chinese Academy of Sciences in 2020. His research focuses on astrodynamics and GNSS data processing.

Jianhua Yang received his Ph.D. degree at the Shanghai Astronomical Observatory, Chinese Academy of Sciences in 2023. His research focuses on precise GNSS data processing.

Xiaogong Hu received his Ph.D. degree from Shanghai Astronomy Observatory in 1999, where he is an associate director at the Center for Astro-geodynamics Research. His research focuses on orbital mechanics of aircraft and applications in satellite navigation and deep space exploration. His current research interests are signal in space service performance of GPS, Galileo, and BDS navigation system.

Chengpan Tang is a senior engineer at the Shanghai Astronomical Observatory, Chinese Academy of Sciences. He received a Bachelor's degree from Central South University in 2011 and a Ph.D. from the Shanghai Astronomical Observatory in 2017. His research focuses on precise GNSS data processing.

Kai Li received his Ph.D. degree at the Shanghai Astronomical Observatory (SHAO), Chinese Academy of Sciences in 2020, and is an engineer at SHAO. His research focuses on precise orbit determination for low earth orbit satellites.

Qingfeng Wu is currently a postgraduate student at the Shanghai Astronomical Observatory, Chinese Academy of Sciences. His main research interests are Precise Orbit Determination and its applications.